AN ASYMPTOTIC INVERSE TO THE KIRCHHOFF-HELMHOLTZ INTEGRAL

M. TYGEL[(*)], J. SCHLEICHER[(*)],
L. T. SANTOS[(*)], AND P. HUBRAL[(**)]

[(*)] Department of Applied Mathematics,

State University of Campinas, IMECC/UNICAMP,

CP 6065, 13081-970 Campinas (SP), Brazil.

[(**)] Geophysical Institute, Karlsruhe University,

Hertzstr. 16, 76187 Karlsruhe, Germany

Campinas, June 21, 1999

ABSTRACT

Modeling a reflected wave by the Kirchhoff-Helmholtz integral consists of an integration along the reflector. By this, one sums the Huygens secondary-source contributions to the wavefield attached to the reflector at the observation point. The proposed asymptotic inverse Kirchhoff-Helmholtz integral, by which this modeling process is inverted, works in a completely analogous way. It consists of an integral along the reflection traveltime surface of the reflector. For a point on the reflector, one sums the reflected-wave contributions attached to the respective reflection-traveltime surface associated with the related source-receiver pair. In this way, the new integral is a more natural inverse to Kirchhoff-Helmholtz forward modeling integral than the conventional Kirchhoff migration integral that is well-known in seismic reflection imaging. The new inverse integral reconstructs the Huygens sources along the reflector, thus providing their positions and amplitudes.

INTRODUCTION

The wavefield originating from a point source and primary-reflected from a smooth reflector overlain by a smooth inhomogeneous acoustic medium can be described by the Kirchhoff integral in the single-scattering, high-frequency approximation (see, e.g., Bleistein, 1984; Frazer and Sen, 1985). The resulting Kirchhoff-Helmholtz integral models the reflected elementary waves as a superposition of Huygens secondary point sources distributed along the reflector. A useful picture of this process is to imagine that the reflector is made up by point-source diffractors that are individually excited by the incoming of the incident wavefield. The intensity of each of these point diffractors along the reflector, regarded a weight in the integral, is specified by the Kirchhoff-Helmholtz approximation. It is given by the product of the incident field and the plane-wave re-

flection coefficient relative to the incident ray that connects the source to the diffraction point, all these quantities being computed at this point. The wavefields radiated by all Huygens point-diffraction sources contribute in form of a constructive interference to the wave measured at the receiver. The asymptotic evaluation of the Kirchhoff-Helmholtz integral leads to the familiar zero-order ray theory approximation (or geometrical optics solution) of the reflected wavefield at the receiver (Tygel et al., 1994, and references therein). Upon proper modification of the weight function along the Kirchhoff-Helmholtz integral, a similar representation integral can be constructed to account for the propagation of diffraction waves at edges and corners at the reflector (see, e.g, Klem-Musatov and Aizenberg, 1985; or Tygel and Ursin, 1999). By independent variation of the locations of the sources and receivers, a multi-coverage experiment can be simulated. In this paper, we will consider data subsets, from sources and receivers combined into pairs according to a chosen measurement configuration. This is typically the situation in seismic data acquisition. In a so-obtained seismogram section, the primary reflections from a given reflector align along the corresponding reflection-traveltime surface. This surface can be interpreted as the kinematic image of the reflector in the seismic record section associated with the chosen configuration. In other words, we can say that this surface implicitly results from the evaluation of the Kirchhoff-Helmholtz integral. In the same way, the wavefield observed along this surface dynamically images the Huygens sources.

The Kirchhoff-Helmholtz integral is largely used to accurately model primary reflections in smooth layered models bounded by smooth interfaces (reflectors). A natural question that arises is whether a transformation exists that performs the opposite task of the Kirchhoff-Helmholtz integral. In other words, this inverse would have to *kinematically and dynamically reconstruct* the reflector. To be consistent with the forward process, this inverse would have to involve a weighted superposition of the observed elementary wave along the reflection traveltime surface of the searched-for reflector. To

3

kinematically and dynamically reconstruct the reflector means to asymptotically recover the reflector location together with the plane-wave reflection coefficient in each point of the reflector. In seismics, this is commonly called the *true amplitude* at all reflector points.

The problem of reconstructing a subsurface reflector out of seismic reflection records on a given configuration is called in the seismic literature the *depth-migration problem* (see, e.g., Stolt, 1978). The depth migration method that is traditionally accepted as a practical inverse (or adjoint) to the Kirchhoff-Helmholtz integral is Kirchhoff depth migration (Porter, 1970; Schneider, 1978; Burridge and Beylkin, 1988; de Hoop and Bleistein, 1997). It is realized by summing the contributions of the reflection data along auxiliary diffraction surfaces constructed on an a priori given reference model. The basic idea of Kirchhoff depth migration is that points on the reflector give rise to diffraction traveltime surfaces, constructed in the reference model, that are tangent to the corresponding observed primary reflection traveltime surfaces. Because of phase coherence along the tangential region, the summation process accumulates constructively interfering signals. In this way, it provides a significantly larger amplitude than the counterpart amplitudes that are obtained when the summation process is carried out for point-diffraction surfaces away from the reflectors. Each diffraction traveltime surface refers to a specific point in depth, on which the resulting summed amplitude is assigned. Performing the above procedure to a fine grid on depth provides the subsurface depth-migration image.

From the above descriptions of the Kirchhoff-Helmholtz integral and Kirchhoff depth migration, we readily realize that both methods are structurely very different. The former is a *modeling process* that uses the actual reflector as a superposition integral. The latter is an *imaging process* that superposes the data along prescribed surfaces constructed on a reference model. As shown in Hubral et al. (1996) and Tygel et al. (1996),

Kirchhoff depth migration is the (asymptotic) inverse of a different operation called *Kirchhoff demigration*, realized by summation along depth-domain surfaces (isochrons) constructed on the same reference model.

So far, the Kirchhoff-Helmholtz integral, a summation operator along a given reflector, lacks a structurely similar (asymptotic) inverse operation. This should have the form of a summation operation along the reflection traveltime corresponding to the reflector, assuming, of course, the same configuration of source-receiver pairs.

This is being set up in this paper by exploring the dual properties between the given reflector and its corresponding traveltime surface. The resulting new inverse Kirchhoff-Helmholtz integral is then completely analogous to the well-known forward-modeling Kirchhoff-Helmholtz integral.

FORMULATION OF THE PROBLEM

To formulate the Kirchhoff-Helmholtz integral transformation pair, we make the following assumptions about the model, as well as some basic properties of the 3-D wave-propagation involved. A fixed global 3-D Cartesian $(\boldsymbol{x}, z)$ coordinate system is assumed throughout. Here, $\boldsymbol{x}$ denotes the 2-D, horizontal coordinate vector and z is the vertical coordinate increasing in the downward direction.

- Referring to Figure 1, we assume the model to consist of a smoothly varying inhomogeneous acoustic medium, bounded above and below by two smooth surfaces. The upper one is the measurement surface and the lower one is the target reflector, to which we will simply refer as Σ. For simplicity, we suppose that the measurement surface coincides with the horizontal plane $z = 0$. The reflector Σ is, also for simplicity, assumed to be parameterized as $z = \Sigma(\boldsymbol{x})$, in which $\boldsymbol{x}$ varies on a given planar set E, called the spatial aperture of the reflector. Points on the

reflector will be generally denoted by $M_\Sigma = M_\Sigma(\boldsymbol{x}) = (\boldsymbol{x}, z = \Sigma(\boldsymbol{x}))$ with $\boldsymbol{x}$ in E.

- A dense distribution of sources and receivers is specified in a certain area of the planar measurement surface $z = 0$. The sources and receivers are grouped in pairs as described by the measurement configuration involved. The locations of the source-receiver pairs are given as a function of a two-dimensional vector parameter $\boldsymbol{\xi}$ that varies in a given planar set A, called the configuration aperture. In other words, each source at point $S = S(\boldsymbol{\xi}) = (\boldsymbol{x}_S(\boldsymbol{\xi}), 0)$ corresponds to exactly one receiver at position $G = G(\boldsymbol{\xi}) = (\boldsymbol{x}_G(\boldsymbol{\xi}), 0)$ with $\boldsymbol{\xi}$ in A.

- For each source-receiver pair (S, G), we suppose that there exists one and only one point $M_\Gamma = M_\Gamma(\boldsymbol{\xi}) = M_\Sigma(\boldsymbol{x}_\Gamma(\boldsymbol{\xi}))$ on the reflector Σ, for which the composite ray $SM_\Gamma G$ constitutes a specular primary reflection. The dependency $\boldsymbol{x}_\Gamma = \boldsymbol{x}_\Gamma(\boldsymbol{\xi})$ implies that the location of the specular reflection point M_Γ is determined by the location of the source-receiver pair (S, G), which in turn is specified by $\boldsymbol{\xi}$. We will denote by $\mathcal{R}(M_\Gamma)$ the plane-wave reflection coefficient for the ray $SM_\Gamma G$ at M_Γ.

- The function $t = \Gamma(\boldsymbol{\xi})$, for varying $\boldsymbol{\xi}$ in A, describes the reflection traveltime from the source $S(\boldsymbol{\xi})$ to the receiver $G(\boldsymbol{\xi})$ along the primary-reflection ray $SM_\Gamma G$. This function is called the reflection-traveltime surface Γ of the reflector Σ. Both surfaces are said to be dual of each other. Points on the traveltime surface Γ will be denoted by $N_\Gamma = N_\Gamma(\boldsymbol{\xi}) = (\boldsymbol{\xi}, t = \Gamma(\boldsymbol{\xi}))$.

- For each point M_Σ on the reflector Σ, we correspondingly assume that there exists one and only one source-receiver pair (S_Σ, G_Σ) for which the composite ray $S_\Sigma M_\Sigma G_\Sigma$ pertains to a specular primary reflection at M_Σ. This pair (S_Σ, G_Σ) is parameterized by the unique parameter value $\boldsymbol{\xi}_\Sigma = \boldsymbol{\xi}_\Sigma(\boldsymbol{x})$, which depends on the horizontal coordinate $\boldsymbol{x}$ of M_Σ. We will denote by $\mathcal{R}(M_\Sigma)$ the plane-wave reflection coefficient for the ray $S_\Sigma M_\Sigma G_\Sigma$ at M_Σ. Also, the notation $N_\Sigma = N_\Sigma(\boldsymbol{x}) = N_\Gamma(\boldsymbol{\xi}_\Sigma(\boldsymbol{x}))$ will be

6

used for a point on Γ pertaining to $\boldsymbol{\xi}_\Sigma$, i.e., to the fixed source-receiver pair (S_Σ, G_Σ).

- At any specified point S, on the measurement surface $z = 0$, we will consider an exploding point source with a certain source signal that is the same for all sources under consideration. Its time dependence can be described by an analytic pulse $F(t)$ that may have a limited bandwidth. The effects of limited bandwidth, however, do not influence the analysis carried out in this paper and need not be considered here. Therefore, we will omit the dependency on $F(t)$ and use the delta function, $\delta(t)$ as the source pulse. We remind that to find the response of a source pulse $F(t)$ we only need to convolve the result with this pulse function.

Under the above assumptions, the zero-order ray-theory provides the following description of a primary reflected elementary wave: For every source-receiver pair (S, G) specified by $\boldsymbol{\xi}$, the reflection event at the receiver is described in analytic form by

$$K_\Gamma(\boldsymbol{\xi}, t) = \mathcal{A}(N_\Gamma)\, \delta(t - \Gamma(\boldsymbol{\xi}))\,, \tag{1}$$

where $\mathcal{A}(N_\Gamma)$ is the amplitude found in the seismic trace at $N_\Gamma = (\boldsymbol{\xi}, t = \Gamma(\boldsymbol{\xi}))$. It is given by

$$\mathcal{A}(N_\Gamma) = \frac{\mathcal{R}(M_\Gamma)}{\mathcal{L}(M_\Gamma)}\,. \tag{2}$$

In the above formula, the amplitude factors $\mathcal{R}(M_\Gamma)$ and $\mathcal{L}(M_\Gamma)$ are the plane-wave reflection coefficient at M_Γ and the geometrical-spreading factor pertaining to the specular reflection ray $SM_\Gamma G$.

We see that $K_\Gamma(\boldsymbol{\xi}, t)$ is aligned along the reflection-traveltime surface Γ as defined above. We may say that $K_\Gamma(\boldsymbol{\xi}, t)$ is the image of the reflector Σ in the time domain under the given measurement configuration. In other words, the image $K_\Gamma(\boldsymbol{\xi}, t)$ describes what we can observe about the reflector in the recorded reflected wavefield.

7

We next introduce the function $I_\Sigma(\boldsymbol{x}, z)$, which is aligned along the reflector Σ according to the formula

$$I_\Sigma(\boldsymbol{x}, z) = \mathcal{R}(M_\Sigma)\, \delta(z - \Sigma(\boldsymbol{x}))\,, \tag{3}$$

The function $I_\Sigma(\boldsymbol{x}, z)$ in equation (3) is very much related to the *singular function of the reflector*, introduced by Cohen and Bleistein (1979). It is defined here, however, in a true-amplitude sense, i.e., with the varying reflection coefficient along the reflector as its amplitude. For that reason, it will be called the *true-amplitude singular function of the reflector* Σ. In the same way, the function $K_\Gamma(\boldsymbol{\xi}, t)$ in equation (3) will be referred to as the *true-amplitude singular function of the reflection-traveltime surface* Γ.

The function $I_\Sigma(\boldsymbol{x}, z)$ can be conceived as the result of a true-amplitude depth migration (Schleicher et al., 1993) of the time-domain reflector image $K_\Gamma(\boldsymbol{\xi}, t)$. Analogously, the function $K_\Gamma(\boldsymbol{\xi}, t)$ can be conceived as the result of a true-amplitude demigration (Hubral et al., 1996) of the depth-domain reflector image $I_\Sigma(\boldsymbol{x}, t)$.

Due to the above observations, we may state that each point N_Γ on Γ is associated to a single point M_Γ on Σ and each point M_Σ on Σ is associated to a single point N_Σ on Γ. The relation between these points is established upon the consideration of the two corresponding specular reflection rays $SM_\Gamma G$ and $S_\Sigma M_\Sigma G_\Sigma$, respectively. Thus, points on Σ and Γ enjoy a *duality* relationship. The two fundamental singular functions $I_\Sigma(\boldsymbol{x}, t)$ and $K_\Gamma(\boldsymbol{\xi}, t)$ can, correspondingly, be called *dual* functions of each other. Tygel et al. (1995) have shown that other useful duality relationships also exist between the above functions (see Appendix A for a brief description). These relations will be needed to derive the inverse Kirchhoff-Helmholtz integral.

Diffraction traveltimes and spatial isochrons

For arbitrary vector parameters $\boldsymbol{\xi}$ in A and arbitrary subsurface points $M = (\boldsymbol{x}, z)$, we introduce the *diffraction traveltime* surface

$$t = \mathcal{T}(\boldsymbol{\xi}, \boldsymbol{x}, z) = \mathcal{T}(\boldsymbol{\xi}, M) = T(S(\boldsymbol{\xi}), M) + T(G(\boldsymbol{\xi}), M) \, , \qquad (4)$$

namely the sum of traveltimes from the source and receiver pair specified by $\boldsymbol{\xi}$ to the subsurface point M. The above formula expresses the traveltimes from the *diffractor point M* to the source-receiver pairs specified by varying $\boldsymbol{\xi}$. This explains the adopted terminology.

The reflection traveltime surface $t = \Gamma(\boldsymbol{\xi})$ of the given reflector Σ can be, as a consequence, recast as

$$t = \Gamma(\boldsymbol{\xi}) = \mathcal{T}(\boldsymbol{\xi}, M_\Gamma) = \mathcal{T}(\boldsymbol{\xi}, \boldsymbol{x}_\Gamma, \Sigma(\boldsymbol{x}_\Gamma)) \, , \qquad (5)$$

where the horizontal vector coordinate $\boldsymbol{x}_\Gamma = \boldsymbol{x}_\Gamma(\boldsymbol{\xi})$ locates the reflection point $M_\Gamma = (\boldsymbol{x}_\Gamma, \Sigma(\boldsymbol{x}_\Gamma))$ on Σ in dependence on the source-receiver pair specified by $\boldsymbol{\xi}$.

We next consider the spatial counterparts of the traveltime functions defined above. For any $\boldsymbol{x}$ in E and arbitrary points $N = (\boldsymbol{\xi}, t)$ in the record space, we introduce the *isochron* function $z = \mathcal{Z}(\boldsymbol{x}, \boldsymbol{\xi}, t)$. This surface is the locus of depth points $M_\mathcal{Z}$ for which the diffraction traveltimes to the source-receiver pairs specified by varying $\boldsymbol{\xi}$ equal the given traveltime t. This is the reason for the terminology isochron (equal time) function. In symbols, points $M_\mathcal{Z} = (\boldsymbol{x}, \mathcal{Z}(\boldsymbol{x}, \boldsymbol{\xi}, t))$ on the isochron are *implicitly* defined by the condition

$$\mathcal{T}(\boldsymbol{\xi}, M_\mathcal{Z}) = T(S(\boldsymbol{\xi}), M_\mathcal{Z}) + T(G(\boldsymbol{\xi}), M_\mathcal{Z}) = t \, . \qquad (6)$$

We assume throughout this paper that for all $\boldsymbol{x}$ in E, for all $\boldsymbol{\xi}$ in A and for all t under consideration, isochrons $z = \mathcal{Z}(\boldsymbol{x}, \boldsymbol{\xi}, t)$ defined by condition (6) exist as unique, smooth

functions. This, of course should impose restrictions on the shape of the reflector, as well as on the measuring configuration. These matters will not be addressed in the present work.

An important observation is that the reflector function $z = \Sigma(\boldsymbol{x})$ can be recast as a restriction of the above isochron function, namely

$$z = \Sigma(\boldsymbol{x}) = \mathcal{Z}(\boldsymbol{x}, N_\Sigma) = \mathcal{Z}(\boldsymbol{x}, \boldsymbol{\xi}_\Sigma, \Gamma(\boldsymbol{\xi}_\Sigma)) \,, \tag{7}$$

where $\boldsymbol{\xi}_\Sigma = \boldsymbol{\xi}_\Sigma(\boldsymbol{x})$ is the vector parameter that specifies the source-receiver pair S_Σ and G_Σ for which the two ray segments $S_\Sigma M_\Sigma$ and $M_\Sigma G_\Sigma$ constitute a reflection ray.

As described in Tygel et al. (1995) and briefly reviewed in Appendix A, diffraction-tion traveltime surfaces $t = \mathcal{T}(\boldsymbol{\xi}, \boldsymbol{x}, \Sigma(\boldsymbol{x}))$, for fixed $\boldsymbol{x}$, and isochron surfaces $z = \mathcal{Z}(\boldsymbol{x}, \boldsymbol{\xi}, \Gamma(\boldsymbol{\xi}))$ for fixed $\boldsymbol{\xi}$ are connected by duality relationships. The diffraction-traveltime surface for a fixed point $M_\Sigma(\boldsymbol{x})$ is tangent to Γ at the (supposedly unique) point $N_\Sigma(\boldsymbol{x}) = N_\Gamma(\boldsymbol{\xi}_\Sigma(\boldsymbol{x}))$ defined by ray $S_\Sigma M_\Sigma G_\Sigma$ as explained above. We call N_Σ the dual point to M_Σ. Correspondingly, the isochron surface for a fixed point $N_\Gamma(\boldsymbol{\xi})$ on Γ is tangent to Σ at the (supposedly unique) point $M_\Gamma(\boldsymbol{\xi}) = M_\Sigma(\boldsymbol{x}_\Gamma(\boldsymbol{\xi}))$. We call M_Γ the dual point to N_Γ. Note that the duality relationship is reciprocal, i.e., $\boldsymbol{x}_\Gamma(\boldsymbol{\xi}_\Sigma(\boldsymbol{x})) = \boldsymbol{x}$ and $\boldsymbol{\xi}_\Sigma(\boldsymbol{x}_\Gamma(\boldsymbol{\xi})) = \boldsymbol{\xi}$. In other words, $M_\Gamma = M_\Sigma$ if and only if $N_\Gamma = N_\Sigma$. Further relationships between the inclinations and curvatures of Σ and Γ at a pair of dual points are established in Appendix A.

THE KIRCHHOFF-HELMHOLTZ INTEGRAL PAIR

In this section, we analyze the forward Kirchhoff-Helmholtz integral geometrically and analytically with the aim of constructing its structurally equivalent inverse in the most natural way.

The forward Kirchhoff-Helmholtz integral

Let be given the one-reflector model and source-receiver specification as described
in the previous sections. The reflected response $K(\boldsymbol{\xi}, t)$ of the acoustic reflector Σ due
to a δ-type point source at $S(\boldsymbol{\xi})$ and observed at the receiver $G(\boldsymbol{\xi})$, can be modeled by
the classical forward KH integral (Frazer and Sen, 1985; Tygel et al., 1994)

$$K(\boldsymbol{\xi}, t) = \frac{1}{4\pi} \int d\Sigma \, \mathcal{W}_K(\boldsymbol{\xi}, M_\Sigma) \, \mathcal{R}_S(M_\Sigma) \, \partial_\eta \delta(t - \mathcal{T}(\boldsymbol{\xi}, M_\Sigma)) \, . \tag{8}$$

In this surface integral over the reflector Σ, $\mathcal{R}_S(M_\Sigma)$ denotes the plane-wave reflection
coefficient of the *incident* ray that connects the source $S(\boldsymbol{\xi})$ to the point M_Σ on the
reflector. Moreover, ∂_η denotes the partial derivative in the direction of the normal $\boldsymbol{\eta}$
to the surface Σ at M_Σ. Finally, $\mathcal{W}_K(\boldsymbol{\xi}, M_\Sigma)$ is the weight function

$$\mathcal{W}_K(\boldsymbol{\xi}, M_\Sigma) = \frac{1}{\mathcal{L}_S(M_\Sigma) \, \mathcal{L}_G(M_\Sigma)} \, , \tag{9}$$

where $\mathcal{L}_S(M_\Sigma)$ and $\mathcal{L}_G(M_\Sigma)$ denote the point-source geometrical-spreading factors along
the two ray segments from the source S to the point M_Σ and from there to the receiver
G. The asymptotic evaluation of the KH integral can be shown to produce the true-
amplitude singular function $K_\Gamma(\boldsymbol{\xi}, t)$ of the traveltime surface Γ (see, e.g., Tygel et al.,
1994). This is briefly reviewed in Appendix B.

As mentioned before, the KH integral expresses the wavefield observed at $G(\boldsymbol{\xi})$ as
a superposition of the wavefields produced by diffraction point sources distributed at
the reflector. These are excited by the incidence point-source wavefield that originates
from $S(\boldsymbol{\xi})$. The use of plane-wave reflection coefficients $\mathcal{R}_S(M_\Sigma)$ is based on the physical
idea that, at each reflector point M_Σ on the reflector, the incident wavefront and the
reflector can be approximated by their respective tangent planes.

For reasons that will become clear later, it is useful to consider a modified ver-
sion of the classical KH integral. As we will see below, integral (8) does not change

11

its asymptotic value if we replace the plane-wave reflection coefficient $\mathcal{R}_S(M_\Sigma)$ of the incident ray segment SM_Σ by the specular reflection coefficient $\mathcal{R}(M_\Sigma)$ that pertains to the reflection ray determined by M_Σ as introduced above. The reason is that at the stationary point of integral (8), both are identical. Thus, we may approximate $K(\boldsymbol{\xi}, t)$ by

$$K(\boldsymbol{\xi}, t) \simeq \frac{1}{4\pi} \int d\Sigma \, \mathcal{W}_K(\boldsymbol{\xi}, M_\Sigma) \, \mathcal{R}(M_\Sigma) \, \partial_\eta \delta(t - \mathcal{T}(\boldsymbol{\xi}, M_\Sigma)) \,. \tag{10}$$

As shown in Appendix B, the asymptotic evaluations of both the KH integral (8) and its modified version (10) produce the true-amplitude singular function $K_\Gamma(\boldsymbol{\xi}, t)$ of the traveltime surface Γ.

It should be noted that, besides being based on a more intuitive physical idea, the classical KH integral, is certainly much better suited for actual computations. This is because the use of the stationary value of the reflection coefficient $\mathcal{R}(M_\Sigma)$ would require a costly determination of the reflection ray that pertains to each point M_Σ on the reflector, which is avoided in the classical KH integral. The modified KH integral (10), however, is worthwhile to consider from a theoretical point of view, because it provides an immediate (asymptotic) transformation link between the true-amplitude singular functions of the reflector Σ and of its corresponding traveltime surface Γ. This link will be the key to the determination of the inverse KH integral.

Note also that the amplitude of the function to be integrated is just the amplitude of the singular function $I_\Sigma(\boldsymbol{x}, t)$ of the reflector. In asymptotic evaluation, where the normal derivative of $\mathcal{R}(M_\Sigma)$ can be neglected, the integrand of equation (10) is nothing else than the normal derivative of the singular function $I_\Sigma(\boldsymbol{x}, t)$ of the reflector, multiplied with a weight function.

As an important step to design an asymptotic inverse KH integral, let us now interpret integral (10) geometrically. Referring to Figure 2, we consider a certain fixed value $\boldsymbol{\xi} = \boldsymbol{\xi}_R$, where we want to compute the modified KH integral (10) as a function

12

of time. Clearly, $\boldsymbol{\xi}_R$ defines a point $N_R = N_\Gamma(\boldsymbol{\xi}_R) = (\boldsymbol{\xi}_R, \Gamma(\boldsymbol{\xi}_R))$ on Γ. Let (S_R, G_R) be the unique source-receiver pair specified by $\boldsymbol{\xi}_R$. We denote by M_R the (supposedly unique) reflection point on Σ which pertains to the source-receiver pair (S_R, G_R), i.e., $M_R = M_\Sigma(\boldsymbol{x}_R)$, where $\boldsymbol{x}_R = \boldsymbol{x}_\Gamma(\boldsymbol{\xi}_R)$. Obviously, M_R is the dual point to N_R, i.e., also $M_R = M_\Gamma(\boldsymbol{\xi}_R)$. The point M_R, on its turn, defines a diffraction traveltime surface that is tangent to the reflection traveltime surface Γ at a supposedly unique point. This tangent point is again point N_R, the dual point to M_R, i.e., $N_R = N_\Sigma(\boldsymbol{x}_R)$. Note that the traveltime surface Γ (dashed line in Figure 2 is a priori unknown. It will become known only by a repeated execution of integral (10) for all $\boldsymbol{\xi}$ in A.

For each point M_Σ on the reflector, the integrand in equation (10) contributes to the final response $K(\boldsymbol{\xi}_R, t)$ at a single point $N_K = (\boldsymbol{\xi}_R, \mathcal{T}(\boldsymbol{\xi}_R, M_\Sigma))$. Recall that $\mathcal{T}(\boldsymbol{\xi}_R, M_\Sigma)$ is defined in equation (4) as the sum of traveltimes along the ray segments $S_R M_\Sigma$ and $M_\Sigma G_R$. In other words, N_K is the point where the diffraction traveltime surface $t = \mathcal{T}(\boldsymbol{\xi}, M_\Sigma)$, cuts the vertical line at $\boldsymbol{\xi}_R$ (see Figure 2). The surface $t = \mathcal{T}(\boldsymbol{\xi}, M_\Sigma)$ is given by all traveltimes along the rays from any source-receiver pair (S, G) to point M_Σ.

The point N_K will fall onto Γ, i.e., it will coincide with point N_R, the dual point to M_R, when M_Σ coincides with M_R. At N_R, the diffraction traveltime surface of M_R, $t = \mathcal{T}(\boldsymbol{\xi}, M_R)$, is tangent to Γ. Due to our assumption that the reflector Σ is continuous and smooth, we thus have a stationary situation at N_R, which means that the main contribution of the integrand in equation (10) will be observed at that point. In other words, the modified KH integral (10) transforms the singular function of reflector Σ onto its image at Γ. The weight function $\mathcal{W}_K(\boldsymbol{\xi}, M_\Sigma)$, computed at $\boldsymbol{\xi} = \boldsymbol{\xi}_R$, serves to perform this transformation in a dynamically correct way, i.e., yielding the correct wave amplitude and pulse shape at N_R.

The inverse Kirchhoff-Helmholtz integral

To set up an analogous integral that achieves the inverse task, namely to reconstruct the singular function of the reflector Σ from its image at Γ, our strategy will be to substitute in the above modified KH integral (10) all points and surfaces by their respective duals. This is geometrically described with the help of Figure 3.

The new KH inverse will consist of an integration along the reflection-traveltime surface Γ, as opposed to its KH forward counterpart (10) that involves an integration along the reflector Σ. In analogy with the preceding construction, we consider the output of the integration at a certain, fixed coordinate $\boldsymbol{x} = \boldsymbol{x}_R$, which determines a point $M_R = M_\Sigma(\boldsymbol{x}_R)$ on Σ. By means of a reflection ray, it also determines a dual point $N_R = N_\Sigma(\boldsymbol{x}_R) = N_\Gamma(\boldsymbol{\xi}_R)$ on Γ. Here, the value of the parameter $\boldsymbol{\xi}_R$ is given by $\boldsymbol{\xi}_R = \boldsymbol{\xi}_\Sigma(\boldsymbol{x}_R)$. The isochron of N_R will be tangent to Σ at $M_R = M_\Gamma(\boldsymbol{\xi}_R)$.

For each point N_Γ on Γ, the new integrand should contribute to the output result $I(\boldsymbol{x}_R, z)$ at a single point M_I, namely the intersection between the isochron of N_Γ, $z = \mathcal{Z}(\boldsymbol{x}, N_\Gamma)$, and the vertical line at $\boldsymbol{x}_R$. In symbols, $M_I = (\boldsymbol{x}_R, \mathcal{Z}(\boldsymbol{x}_R, N_\Gamma))$.

The point M_I will fall on Σ, i.e., it will coincide with M_R, when N_Γ coincides with N_R, the dual point of M_R. At M_R, the isochron $z = \mathcal{Z}(\boldsymbol{x}, N_R)$ is tangent to Σ. Due to our assumptions of a smooth reflector and uniqueness of dual points, we have again the situation of an isolated stationary point at M_R, which means that the main contribution of the new integral will be observed at M_R. As before, the reflector Σ (dashed line in Figure 3) is a priori unknown. It will become known only by a repeated execution of the above process for all $\boldsymbol{x}$ in E. In this way, we have geometrically constructed a kinematic transformation of the reflection-traveltime function Γ into the reflector Σ.

In the same way as the amplitude of the function to be integrated in equation (10) is that of the singular function $I_\Sigma(\boldsymbol{x}, z)$ of the reflector, multiplied with an appropriate

weight function, it is most natural to set the amplitude of the integrand in the inverse integral to be that of the singular function $K_\Gamma(\boldsymbol{\xi}, t)$ of the reflection-traveltime surface Γ, multiplied with a corresponding, yet unspecified weight function. Analogously to the weight function $\mathcal{W}_K(\boldsymbol{\xi}, M_\Sigma)$ in the forward KH integral (10), the new weight function, $\mathcal{W}_I(\boldsymbol{x}, N_\Gamma)$, will be included into the inverse integral in order to assure that also this inverse transformation can be performed in a dynamically correct way, i.e., to correctly reconstruct the varying reflection coefficient along the reflector Σ. Similarly to the forward KH integral, the correct pulse shape will be ensured by the use of a derivative of the involved δ-pulse in the direction normal to Γ.

Translating the above arguments into mathematical terms and in full correspondence to the modified KH integral (10), we can now set up the proposed inverse KH integral as

$$I(\boldsymbol{x}, z) = -\frac{1}{4\pi} \int d\Gamma \; \mathcal{W}_I(\boldsymbol{x}, N_\Gamma) \; \mathcal{A}(N_\Gamma) \; \partial_\mu \delta(z - \mathcal{Z}(\boldsymbol{x}, N_\Gamma)) \;. \tag{11}$$

In this formula, ∂_μ denotes, correspondingly to ∂_η in equation (10), the partial derivative in the direction of the normal $\boldsymbol{\mu}$ to the traveltime surface Γ at the generic point $N_\Gamma = (\boldsymbol{\xi}, \Gamma(\boldsymbol{\xi}))$ that describes the integral. The point N_Γ, by means of the configuration parameter $\boldsymbol{\xi}$, automatically determines the source-receiver pair (S, G), where $S = S(\boldsymbol{\xi})$ and $G = G(\boldsymbol{\xi})$. As previously, let us denote by M_R the (unique) specular reflection point on the reflector pertaining to the source-receiver pair (S, G) defined by $\boldsymbol{\xi}$. From the analysis carried out in Appendix B, it follows that the weight function can be selected as

$$\mathcal{W}_I(\boldsymbol{x}, N_\Gamma) = \frac{h_B(\boldsymbol{\xi}, M_I) \; v^3(M_I) \; \cos^2 \theta(M_I)}{\cos^2 \alpha(M_I)} \mathcal{L}_S(M_I) \mathcal{L}_G(M_I) \;. \tag{12}$$

Here, M_I is the point $(\boldsymbol{x}, z = \mathcal{Z}(\boldsymbol{x}, N_\Gamma))$, where the isochron $z = \mathcal{Z}(\boldsymbol{x}, N_\Gamma)$ of N_Γ cuts the vertical line at M_R (see Figure 3). Also, $v(M_I)$ is the medium velocity at M_I and $\mathcal{L}_S(M_I)$ and $\mathcal{L}_G(M_I)$ are the point-source geometrical-spreading factors along the ray

segments SM_I and M_IG, respectively. Moreover, $\theta(M_I)$ represents the angle the normal to Γ at N_Γ makes with the vertical t-axis), and $\alpha(M_I)$ denotes the incidence angle that the incoming ray SM_I makes with the isochron normal at M_I (see Figure 3). Finally, $h_B(\boldsymbol{\xi}, M_I)$ is the modulus of the Beylkin determinant (Beylkin, 1985; Bleistein, 1987),

$$h_B(\boldsymbol{\xi}, M_I) = \begin{bmatrix} \boldsymbol{\nabla} \mathcal{T}(\boldsymbol{\xi}, M_I) \\ \partial_{\xi_1} \boldsymbol{\nabla} \mathcal{T}(\boldsymbol{\xi}, M_I) \\ \partial_{\xi_2} \boldsymbol{\nabla} \mathcal{T}(\boldsymbol{\xi}, M_I) \end{bmatrix} , \tag{13}$$

where $\boldsymbol{\nabla} = (\partial_{x_1}, \partial_{x_2}, \partial_z)$ is the spatial gradient operator.

As shown in Appendix B, the forward KH integrals (8) and (10), as well as the new inverse KH integral (11), can be asymptotically evaluated by the time-domain version of the standard stationary-phase method, as described, e.g., in Bleistein (1984). The KH forward integrals (8) and (10) can be approximated, for time values $t \approx \Gamma(\boldsymbol{\xi})$ as

$$K(\boldsymbol{\xi}, t) \approx K_\Gamma(\boldsymbol{\xi}, t) = \mathcal{A}(N_\Gamma) \, \delta(t - \Gamma(\boldsymbol{\xi})) , \tag{14}$$

namely, the true-amplitude singular function of the traveltime surface Γ.

Correspondingly, the new KH inverse integral (11) can be asymptotically approximated for spatial values $z \approx \Sigma(\boldsymbol{x})$ as

$$I(\boldsymbol{x}, z) \approx I_\Sigma(\boldsymbol{x}, z) = \mathcal{R}(M_\Sigma) \, \delta(z - \Sigma(\boldsymbol{x})) , \tag{15}$$

i.e., the true-amplitude singular function of the reflector Σ.

This means that integral (11) is the (asymptotic) inverse to the modified KH integral (10), and thus also to the classical forward KH integral (8), since the latter is asymptotically equivalent to integral (10). The integrals (8) (or (10)) and (11) form an asymptotic transform pair between the depth-domain true-amplitude singular function $I_\Sigma(\boldsymbol{x}, z)$ of the reflector Σ and its corresponding time-domain true-amplitude singular function $K_\Gamma(\boldsymbol{\xi}, t)$ of the traveltime surface Γ.

16

A simple numerical example

To verify the validity of the inverse Kirchhoff-Helmholtz integral (11), we have designed the following simple numerical experiment. A seismic common-offset experiment with a half-offset of $h = 500$ m was simulated above the earth model depicted in Figure 4. It consists of two homogeneous acoustic layers with constant velocities of 4 km/s and 4.5 km/s, respectively, separated by a smooth interface in the form of a dome structure. The terminology "common-offset experiment" means that all source-receiver pairs involved are separated by the same fixed offset of $2h = 1000$ m. More specifically, the location of each source and each receiver can be expressed as $x_S = \xi - h$ and $x_G = \xi + h$, where parameter ξ is the midpoint coordinate, i.e., $\xi = (x_S + x_G)/2$.

Figure 5a shows the common-offset data as modeled by the forward integral (8). For an easier analysis, we have convolved the results of integral (8) with a Ricker wavelet of unit peak amplitude and a duration of 64 ms. Also indicated in Figure 5a is the reflection traveltime curve as the locus of the peak amplitudes of the time-symmetric Ricker wavelet used in the numerical modeling. Along this identified traveltime curve, we now perform the new inverse Kirchhoff-Helmholtz integral (11). The result is shown in Figure 5b. The inversion results show that the obtained wavelets align perfectly along the reflector that is indicated by a continuous line. This confirms that integral (11) performs the inversion task in a kinematically correct way (i.e., it correctly positions the reflector in depth).

To check on the dynamics, we determine the obtained peak amplitudes and compare them to the correct reflection coefficient (see Figure 6a). We observe an almost perfect coincidence between the inverted amplitudes (thin line) and the theoretical curve (bold line) within the center region of the dome structure. On both flanks, a slightly larger error can be observed. This is due to the reduced illumination of this part of

the reflector, caused by the employed measurement configuration. In Figure 6b, this observation is quantified by the relative error of the observed amplitudes. In the central region, the error does not exceed half a percent. In the less well-illuminated parts of the reflector, we still have errors less than four percent, an also good amplitude recovery. These results (and other numerical experiments not shown in this paper) confirm our claim that integral (11) constitutes indeed an asymptotic inverse to the well-known forward Kirchhoff-Helmholtz integral (8).

CONCLUSIONS

We have presented an analogous (asymptotic) inverse to the well-known forward Kirchhoff-Helmholtz (KH) integral. Just as the forward KH integral can be conceived as a superposition of the elementary responses of all Huygens secondary sources along the reflector, we can conceive its inverse as a superposition of "elementary reflection images" along the reflection-traveltime surface. The elementary Huygens sources along the reflector are then recovered in position and strength.

For a given distribution of source-receiver pairs (the measurement configuration) that provides the "illumination" of the reflector, we have introduced the concepts of the true-amplitude singular functions of the reflector and its corresponding reflection-traveltime surface. These are nothing else than δ-functions localized on the two surfaces multiplied by specular reflection coefficients (at the reflector) and zero-order ray responses (at the reflection-traveltime surface). The new KH transform pair provides an (asymptotic) link between the true-amplitude singular functions of the reflector and its reflection-traveltime surface. The new inverse KH integral was constructed using the fundamental dual properties that relate primary-reflection surfaces of the time-domain data space and their corresponding depth-domain reflectors in model space. By a simple numerical example, we have confirmed that the new inverse Kirchhoff-Helmholtz inte-

gral indeed recovers the reflection coefficients along the reflecting interface as claimed theoretically.

The new inverse integral also fills a gap which originates from the observation that the conventional Kirchhoff migration integral (Schneider, 1978), well known in the seismic literature and frequently used to solve the inverse problem, is not an inverse but the adjoint operation to the forward KH integral (Tarantola, 1984). In fact, the structurely correct inverse to Kirchhoff migration has also been recently provided under the name of the Kirchhoff demigration integral (Hubral et al., 1996; Tygel et al., 1996).

The proposed inverse KH integral enables the design of a new seismic migration technique that would deserve the name Kirchhoff migration much more than what is up to now associated with this name. Note, however, that conventional Kirchhoff migration has done an excellent job in practice. Whether the new inverse Kirchhoff-Helmholtz integral can be employed with comparable success in practical seismic inverse problems remains a topic of future research.

ACKNOWLEDGEMENTS

References

Beylkin, G., 1985, Imaging of discontinuities in the inverse scattering problem by inversion of a generalized Radon transform: J. Math. Phys., **26**, 99–108.

Bleistein, N., 1984, Mathematics of wave phenomena, Academic Press.

Bleistein, N., 1987, On the imaging of reflectors in the earth: Geophysics, **52**, 931–942.

Burridge, R., and Beylkin, G., 1988, On double integrals over spheres: Inverse Problems, **4**, 1–10.

Cohen, J.K., and Bleistein, N., 1979, The singular function of a surface and physical optics inverse scattering: Wave Motion, **1**, 153–161.

de Hoop, M.V., and Bleistein, N., 1997, Generalized radon transform inversions in anisotropic elastic media: Inverse Problems, **13**, 669–690.

Frazer, L.N., and Sen, M.K., 1985, Kirchhoff-Helmholtz reflection seismograms in a laterally inhomogeneous multi-layered elastic medium – I. Theory: Geophys. J. Roy. Astr. Soc., **80**, 121–147.

Hubral, P., Schleicher, J., and Tygel, M., 1992, Three-dimensional paraxial ray properties – Part I. Basic relations: J. Seis. Expl., **1**, 265–279.

Hubral, P., Schleicher, J., and Tygel, M., 1996, A unified approach to 3-D seismic reflection imaging – Part I: Basic concepts: Geophysics, **61**, 742–758.

Klem-Musatov, K.D., and Aizenberg, A.M., 1985, Seismic modelling by methods of the theory of edge waves: J. Geophys., **57**, 90–105.

Porter, R.P., 1970, Diffraction-limited scalar image formation with holograms of arbitrary shape: J. Acoust. Soc. Am., **60**, 1051–1059.

Schleicher, J., Tygel, M., and Hubral, P., 1993, 3-D true-amplitude finite-offset migration: Geophysics, **58**, 1112–1126.

Schneider, W.A., 1978, Integral formulation for migration in two and three dimensions: Geophysics, **43**, 49–76.

Stolt, R.H., 1978, Migration by Fourier transform: Geophysics, **43**, 23–48.

Tarantola, A., 1984, Linearized inversion of seismic data: Geophys. Prosp., **32**, 998–1005.

Tygel, M., Schleicher, J., and Hubral, P., 1994, Kirchhoff-Helmholtz theory in modelling and migration: J. Seis. Expl., **3**, 203–214.

Tygel, M., Schleicher, J., and Hubral, P., 1995, Dualities between reflectors and reflection-time surfaces: J. Seis. Expl., **4**, 123–150.

Tygel, M., Schleicher, J., and Hubral, P., 1996, A unified approach to 3-D seismic reflection imaging – Part II: Theory: Geophysics, **61**, 759–775.

Tygel, M., and Ursin, B., 1999, Weak-contrast edge and vertex diffractions in anisotropic elastic media: Wave Motion, **29**, 363–373.

APPENDIX A

Complete Duality Theorems

In this Appendix, we revisit the first and second duality theorems of Tygel et al. (1995) that provide fundamental geometrical relationships between a reflector Σ and its corresponding primary reflection traveltime surface Γ. As these relationships are crucial to the derivation of practically all the results presented in this paper, we find it convenient to briefly state and comment them here.

As established in the text, we consider a given configuration of source-receiver pairs (S, G), specified by their dependence on a vector parameter $\boldsymbol{\xi}$. The family of rays from each S to a corresponding G under reflection from a *reflector* Σ defines the *reflection-traveltime surface* Γ.

The duality theorems to be stated below relate tangents and normals (first-order derivatives) and curvatures (second-order derivatives) of the reflector Σ: $t = \Sigma(\boldsymbol{x})$ and its reflection-traveltime surface Γ: $t = \Gamma(\boldsymbol{\xi})$, called throughout the *fundamental dual surfaces*. The relationships between the fundamental dual surfaces are given in terms of *auxiliary surfaces*, namely the *isochrons* Σ_Γ: $z = \mathcal{Z}(\boldsymbol{x}, N_\Gamma)$ and the *diffraction traveltimes* Γ_Σ: $t = \mathcal{T}(\boldsymbol{\xi}, M_\Sigma)$. Note that the latter are, in an analogous sense, also dual to each other. With the above definitions, we are ready to state the duality theorems.

First duality theorem

(a) For any given point M_Σ on the reflector Σ, its corresponding diffraction traveltime surface Γ_Σ is *tangent* to the reflection traveltime Γ at a unique point N_Σ.
(b) For any given point N_Γ on the reflection traveltime Γ, its corresponding isochron

surface Σ_Γ is *tangent* to the reflector Σ at a unique point M_Γ.

The points M_Σ and N_Σ or M_Γ and N_Γ in (a) and (b) are called *dual points* of each other. From now on, we will refer to an arbitrary pair of dual points M_R and N_R.

(c) For $\boldsymbol{\xi}$ in A and $\boldsymbol{x}$ in E, we define the partial-derivative functions

$$m_D = \partial_z \mathcal{T}(\boldsymbol{\xi}, \boldsymbol{x}, z) \quad \text{and} \quad n_I = \partial_t \mathcal{Z}(\boldsymbol{x}, \boldsymbol{\xi}, t) \ . \tag{A-1}$$

Then, at any pair of dual points

$$m_D \cdot n_I = 1 \ . \tag{A-2}$$

(d) For the dual points M_R and N_R, let S and G denote the source-receiver pair associated to them. Considering the reflection ray SM_RG, let α be the angle the incident ray SM_R makes with the normal of Σ at M_R, let β be the angle between the normal to Σ at M_R and the vertical axis and let v be the velocity of the medium just above M_R. Finally, let θ denote the angle the normal to Γ makes with the t-axis at N_R. Using the same notation as above, the following expressions are valid at the dual points M_R and N_R

$$m_D = \partial_z \mathcal{T} = \frac{2 \cos \alpha_R \cos \beta_R}{v_R} \ , \tag{A-3}$$

$$\partial_\eta \mathcal{T} = \frac{m_D}{\cos \beta_R} = \frac{2 \cos \alpha_R}{v_R} \ , \tag{A-4}$$

and

$$\partial_\mu \mathcal{Z} = \frac{n_I}{v_R \cos \theta_R} = \frac{1}{2 \cos \alpha_R \cos \beta_R \cos \theta_R} \ . \tag{A-5}$$

Here, ∂_η and ∂_μ denote the derivative in the direction of the normals $\boldsymbol{\eta}$ and $\boldsymbol{\mu}$ to the reflector and the reflection-traveltime surface, respectively. Equations (A-4) an (A-5) follow directly from geometrical considerations. Note that the time coordinate axis has to be scaled with the local velocity $v_R = v(M_R)$ in order to have a well-defined normal derivative $\partial_\mu \mathcal{Z}$.

Second duality theorem

Let us introduce the 2×2 spatial Hessian matrices

$$\underset{\sim}{\Sigma}(\boldsymbol{x}) = \left(\frac{\partial^2 \Sigma(\boldsymbol{x})}{\partial x_i \partial x_j} \right) \quad \text{and} \quad \underset{\sim}{\boldsymbol{Z}}(\boldsymbol{x}, \boldsymbol{\xi}, t) = \left(\frac{\partial^2 \mathcal{Z}(\boldsymbol{x}, \boldsymbol{\xi}, t)}{\partial x_i \partial x_j} \right) \qquad \text{(A-6)}$$

of the reflector and isochron, respectively. In the same way, we introduce the 2×2 traveltime Hessian matrices

$$\underset{\sim}{\boldsymbol{\Gamma}}(\boldsymbol{\xi}) = \left(\frac{\partial^2 \Gamma(\boldsymbol{\xi})}{\partial \xi_i \partial \xi_j} \right) \quad \text{and} \quad \underset{\sim}{\boldsymbol{H}}(\boldsymbol{\xi}, \boldsymbol{x}, z) = \left(\frac{\partial^2 \mathcal{T}(\boldsymbol{\xi}, \boldsymbol{x}, z)}{\partial \xi_i \partial \xi_j} \right) \qquad \text{(A-7)}$$

of the reflection and diffraction-traveltime surfaces, respectively. We also introduce the "auxiliary isochron function" $\mathcal{Z}_\Gamma$ as the restriction of the isochron function to points N_Γ on the traveltime surface Γ of the reflector Σ, i.e.,

$$\mathcal{Z}_\Gamma(\boldsymbol{x}, \boldsymbol{\xi}) = \mathcal{Z}(\boldsymbol{x}, N_\Gamma) = \mathcal{Z}(\boldsymbol{x}, \boldsymbol{\xi}, \Gamma(\boldsymbol{\xi})) \qquad \text{(A-8)}$$

with its 2×2 Hessian matrix

$$\underset{\sim}{\boldsymbol{Z}}_\Gamma(\boldsymbol{x}, \boldsymbol{\xi}) = \left(\frac{\partial^2 \mathcal{Z}_\Gamma(\boldsymbol{x}, \boldsymbol{\xi})}{\partial \xi_i \partial \xi_j} \right) \ . \qquad \text{(A-9)}$$

In the same way, we introduce the "auxiliary traveltime function" $\mathcal{T}_\Sigma$ as the restriction of the diffraction traveltime function to points on the reflector, i.e.

$$\mathcal{T}_\Sigma(\boldsymbol{\xi}, \boldsymbol{x}) = \mathcal{T}(\boldsymbol{\xi}, M_\Sigma) = \mathcal{T}(\boldsymbol{\xi}, \boldsymbol{x}, \Sigma(\boldsymbol{x})) \qquad \text{(A-10)}$$

with its 2×2 Hessian matrix

$$\underset{\sim}{\boldsymbol{H}}_\Sigma(\boldsymbol{\xi}, \boldsymbol{x}) = \left(\frac{\partial^2 \mathcal{T}_\Sigma(\boldsymbol{\xi}, \boldsymbol{x})}{\partial x_i \partial x_j} \right) \ . \qquad \text{(A-11)}$$

Additionally, the auxiliary traveltime function $\mathcal{T}_\Sigma$ gives rise to its 2×2 mixed-derivative matrix

$$\underset{\sim}{\boldsymbol{\Lambda}}(\boldsymbol{\xi}, \boldsymbol{x}, z) = \left(\frac{\partial^2 \mathcal{T}_\Sigma(\boldsymbol{\xi}, \boldsymbol{x})}{\partial \xi_i \partial x_j} \right) \ . \qquad \text{(A-12)}$$

Finally, we will also need the 3×3 mixed derivative matrix

$$\underset{\sim}{\boldsymbol{H}}_B(\boldsymbol{\xi}, \boldsymbol{x}, z) = \begin{pmatrix} \nabla_{\boldsymbol{x}} \mathcal{T}(\boldsymbol{\xi}, \boldsymbol{x}, z) \\ \partial_{\xi_1} \nabla_{\boldsymbol{x}} \mathcal{T}(\boldsymbol{\xi}, \boldsymbol{x}, z) \\ \partial_{\xi_2} \nabla_{\boldsymbol{x}} \mathcal{T}(\boldsymbol{\xi}, \boldsymbol{x}, z) \end{pmatrix} \tag{A-13}$$

of the unrestricted diffraction-traveltime function $\mathcal{T}(\boldsymbol{\xi}, \boldsymbol{x}, z)$.

At a pair of dual points M_R and N_R, the second duality theorem states then the following relationships between the above matrices:

$$\underset{\sim}{\boldsymbol{H}} - \underset{\sim}{\boldsymbol{\Gamma}} = \underset{\sim}{\boldsymbol{\Lambda}}\, \underset{\sim}{\boldsymbol{H}}_{\Sigma}^{-1}\, \underset{\sim}{\boldsymbol{\Lambda}}^T \; , \tag{A-14}$$

$$\underset{\sim}{\boldsymbol{H}}_{\Sigma} = m_D \left(\underset{\sim}{\boldsymbol{\Sigma}} - \underset{\sim}{\boldsymbol{Z}} \right) \; , \tag{A-15}$$

and

$$\underset{\sim}{\boldsymbol{Z}}_{\Gamma} = \frac{1}{m_D} \left[\underset{\sim}{\boldsymbol{\Gamma}} - \underset{\sim}{\boldsymbol{H}} \right] = -\frac{1}{m_D} \underset{\sim}{\boldsymbol{\Lambda}}\, \underset{\sim}{\boldsymbol{H}}_{\Sigma}^{-1}\, \underset{\sim}{\boldsymbol{\Lambda}}^T \; . \tag{A-16}$$

Here and in the following, a matrix symbol without argument stands for the respective matrix evaluated at M_R and N_R.

A useful relationship can also be obtained after elimination of $\underset{\sim}{\boldsymbol{H}}_{\Sigma}$ in equations (A-14) and (A-15), namely

$$m_D \left(\underset{\sim}{\boldsymbol{H}} - \underset{\sim}{\boldsymbol{\Gamma}} \right) = \underset{\sim}{\boldsymbol{\Lambda}} \left(\underset{\sim}{\boldsymbol{\Sigma}} - \underset{\sim}{\boldsymbol{Z}} \right)^{-1} \underset{\sim}{\boldsymbol{\Lambda}}^T \; . \tag{A-17}$$

Moreover, we have the additional relationship

$$\det \underset{\sim}{\boldsymbol{\Lambda}} = \frac{\det \underset{\sim}{\boldsymbol{H}}_B}{m_D} \; , \tag{A-18}$$

where $\det \underset{\sim}{\boldsymbol{H}}_B$ is the Beylkin determinant (Beylkin, 1985; Bleistein, 1987). Note that the quantity $h_B = |\det \underset{\sim}{\boldsymbol{H}}_B|$ appears in the weight function (12) of the new inverse KH integral.

It is to be reminded that the first duality theorem and equations (A-14), (A-15), (A-17) and (A-18) have been proved in Tygel et al. (1995). The new equation (A-16)

25

is derived below. With the inclusion of this last equation, we call the above results the complete duality theorems.

Analysis of the isochron: Proof of equation (A-16)

In this section, we present a proof of the new result (A-16) of the second duality theorem. Recalling that $M_{\mathcal{Z}}(\boldsymbol{x}, \boldsymbol{\xi}) = (\boldsymbol{x}, \mathcal{Z}(\boldsymbol{x}, N_\Gamma))$ is a point on the isochron defined by N_Γ, we start from the identity

$$\mathcal{T}(\boldsymbol{\xi}, M_{\mathcal{Z}}(\boldsymbol{x}, \boldsymbol{\xi})) = \Gamma(\boldsymbol{\xi}) . \tag{A-19}$$

Differentiate both sides with respect to ξ_j ($j = 1, 2$) using the chain rule to obtain

$$\frac{\partial \mathcal{T}}{\partial \xi_j} + \partial_z \mathcal{T}(\boldsymbol{\xi}, M_{\mathcal{Z}}) \frac{\partial \mathcal{Z}_\Gamma}{\partial \xi_j} = \frac{\partial \Gamma}{\partial \xi_j} . \tag{A-20}$$

At the stationary point N_R, we have

$$\partial \mathcal{Z}_\Gamma / \partial \xi_j = 0 , \tag{A-21}$$

which leads to the well-known tangency property between the reflection-traveltime and diffraction surfaces

$$\frac{\partial \mathcal{T}}{\partial \xi_j} = \frac{\partial \Gamma}{\partial \xi_j} . \tag{A-22}$$

The above result is nothing else than part (a) of the first duality theorem. We next differentiate both sides of equation (A-20) with respect to ξ_i using again the chain rule. At the stationary point N_R, we find upon the use of the condition (A-21)

$$\frac{\partial^2 \mathcal{T}}{\partial \xi_i \partial \xi_j} + \partial_z \mathcal{T}(\boldsymbol{\xi}, M_R) \frac{\partial^2 \mathcal{Z}_\Gamma}{\partial \xi_i \partial \xi_j} = \frac{\partial^2 \Gamma}{\partial \xi_i \partial \xi_j} . \tag{A-23}$$

Dividing by $m_D = \partial_z \mathcal{T}(\boldsymbol{\xi}, M_R)$, we obtain

$$\frac{\partial^2 \mathcal{Z}_\Gamma}{\partial \xi_i \partial \xi_j} = \frac{1}{m_D} \left[\frac{\partial^2 \Gamma}{\partial \xi_i \partial \xi_j} - \frac{\partial^2 \mathcal{T}}{\partial \xi_i \partial \xi_j} \right] , \tag{A-24}$$

which, in the previous notation, is exactly the left-hand equation of formula (A-16). The right-hand equation follows directly from equation (A-14). The proof is, thus, complete.

APPENDIX B

Asymptotic evaluation of the integrals

The forward and inverse KH integrals can be asymptotically approximated by means of the time-domain version of the standard technique of stationary-phase (see, e.g., Bleistein, 1984) that is designed for the high-frequency evaluation of Fourier-type integrals. By means of these evaluations, the weight expressions of the KH integrals, as stated in the text, will be derived.

Asymptotic evaluation of the forward KH integral

In this section, we asymptotically evaluate the forward KH integral (8) at a fixed point $\boldsymbol{\xi}_R$ (see Figure 2). For that purpose, we translate the high-frequency, stationary-phase results of Bleistein (1984) to the time domain. In this way, the leading term of the asymptotic evaluation of the forward KH integral is readily found to be

$$K_{as}(\boldsymbol{\xi}_R, t) = \frac{\mathcal{R}(M_R)}{2\mathcal{L}_S(M_R)\,\mathcal{L}_G(M_R)\cos\beta_R}\,\frac{e^{i\pi\,(2-\sigma)/4}}{\sqrt{|H_\Sigma|}}\,\partial_\eta \mathcal{T}(\boldsymbol{\xi}_R, M_R)\,\delta(t - \Gamma(\boldsymbol{\xi}_R))\,, \quad \text{(B-1)}$$

where $M_R = M_\Sigma(\boldsymbol{x}_R)$ is the (unique) specular reflection point on the reflector Σ. It pertains to the source-receiver pair specified by the given configuration vector parameter $\boldsymbol{\xi}_R$. Here, $\boldsymbol{x}_R = \boldsymbol{x}_\Gamma(\boldsymbol{\xi}_R)$ is the stationary point of integral (10). Observe that due to the duality, $M_R = M_\Gamma(\boldsymbol{\xi}_R)$. Moreover, β_R is the angle the normal to the reflector makes with the vertical axis at M_R. Finally, σ and H_Σ are the signature and the determinant, respectively, of the Hessian matrix of the auxiliary traveltime $\mathcal{T}_\Sigma(\boldsymbol{\xi}, \boldsymbol{x})$, as defined by equation (A-10), evaluated at $(\boldsymbol{\xi}_R, \boldsymbol{x}_R)$. Note that equation (B-1) is the result of the asymptotic evaluation of *both* the classical forward KH integral (8) *and* its modified version (10), because at the stationary point M_R, we have $\mathcal{R}_S(M_R) = \mathcal{R}(M_R)$.

The matrix $\underset{\sim}{\boldsymbol{H}}_\Sigma$ plays an important role in the investigation of what is the reflector region in the vicinity of the reflection point that mainly contributes under the illumination of a given source-receiver measurement configuration. The projection of this matrix onto the tangent plane to the reflector at the reflection point is referred to as the Fresnel matrix corresponding to this point. As was shown in Hubral et al. (1992), this projected matrix defines the size of the Fresnel zone.

We now recall the fact that (see equation (A-4))

$$\partial_\eta \mathcal{T}(\boldsymbol{\xi}, M_R) = \frac{2\cos\alpha_R}{v_R} \, , \tag{B-2}$$

is nothing else than the well known *obliquity factor* in the classical KH integral. Here, v_R is the local velocity and α_R is the specular reflection angle at M_R. Substituting the above expression into the KH integral asymptotic evaluation (B-1), we can recast it in the form of a zero-order ray theory approximation

$$K_{as}(\boldsymbol{\xi}_R, t) = \frac{\mathcal{R}(M_R)}{\mathcal{L}(M_R)} \, \delta(t - \Gamma(\boldsymbol{\xi}_R)) = \mathcal{A}(N_R) \, \delta(t - \Gamma(\boldsymbol{\xi}_R)) \, . \tag{B-3}$$

Observe that this result is nothing else than the true-amplitude singular function (1) of the reflection-traveltime surface at the chosen point $\boldsymbol{\xi}_R$, thus confirming result (14).

In formula (B-3), one recognizes

$$\mathcal{L}(M_R) = \frac{\mathcal{L}_S(M_R) \, \mathcal{L}_G(M_R) v_R \cos\beta_R}{\cos\alpha_R} \, e^{i\pi \, (\sigma-2)/4} \, \sqrt{|H_\Sigma|} \, , \tag{B-4}$$

as the geometrical-spreading factor of the reflected ray SM_RG. Introducing further the *Fresnel geometrical-spreading factor*

$$\mathcal{L}_F(M_R) = \frac{\cos\alpha_R}{v_R \cos\beta_R} \frac{e^{i\pi \, (2-\sigma)/4}}{\sqrt{|H_\Sigma|}} \, , \tag{B-5}$$

we find the geometrical-spreading decomposition (Tygel et al., 1994)

$$\mathcal{L}(M_R) = \frac{\mathcal{L}_S(M_R) \, \mathcal{L}_G(M_R)}{\mathcal{L}_F(M_R)} \, . \tag{B-6}$$

This formula will be of further use in the evaluation of the inverse KH integral (11).

Asymptotic evaluation of the inverse KH integral

In the same way as the forward KH integral, also the inverse KH integral admits a simple asymptotic evaluation, irrespective of the specific form of the weight function, which will, for the time being, be left unspecified. In this section, we will compare the asymptotic evaluations of both KH integrals to confirm the correct duality of the transformation pair given by equations (8) and (11). The dynamics of the present analysis will, in fact, determine the adequate form of the necessary weight function in integral (11).

The asymptotic evaluation of the inverse KH integral (11) can be obtained using an analogous procedure as the one used for the direct KH counterpart. We find for the leading-order term of the asymptotic evaluation at a certain fixed point $\boldsymbol{x} = \boldsymbol{x}_R$

$$I_{as}(\boldsymbol{x}_R, z) = \mathcal{A}(N_R) \, \frac{\mathcal{W}_I(\boldsymbol{x}_R, N_R)}{2 \cos \theta_R} \frac{e^{-i\pi \, (2+\gamma)/4}}{\sqrt{|Z_\Gamma|}} \, \partial_\mu \mathcal{Z}(\boldsymbol{x}_R, N_R) \, \delta(z - \Sigma(\boldsymbol{x}_R)) \,, \qquad \text{(B-7)}$$

where $N_R = N_\Gamma(\boldsymbol{\xi}_R)$ specifies the source-receiver pair (S_R, G_R) for which the reflector point $M_R = M_\Sigma(\boldsymbol{x}_R) = M_\Gamma(\boldsymbol{\xi}_R)$ is a specular reflection point. Here, $\boldsymbol{\xi}_R = \boldsymbol{\xi}_R(\boldsymbol{x}_R)$ is the stationary point of integral (11). In other words, N_R, on the reflection-traveltime surface Γ, is the dual point to the point M_R on the reflector Σ in the vicinity of which the integral (11) is calculated, i.e., $N_R = N_\Sigma(\boldsymbol{x}_R)$. Finally, γ and Z_Γ are the signature and the determinant, respectively, of the Hessian matrix $\underset{\sim}{\boldsymbol{Z}}_\Gamma$ of the auxiliary isochron function $\mathcal{Z}_\Gamma(\boldsymbol{x}, \boldsymbol{\xi})$, defined by equation (A-8) and evaluated at $(\boldsymbol{x}_R, \boldsymbol{\xi}_R)$. Also, θ_R is the local reflection-traveltime dip at N_R. To find an expression for the determinant Z_Γ of the matrix $\underset{\sim}{\boldsymbol{Z}}_\Gamma$, we make use of the results of the second duality theorem. Taking the determinant of both sides of equation (A-17), we employ employ the equations (A-14)

and (A-18) to find

$$Z_\Gamma = \det \underset{\sim}{\boldsymbol{Z}}_\Gamma = \frac{h_B^2}{m_D^4} \frac{1}{\det \underset{\sim}{\boldsymbol{H}}_\Sigma} = \frac{h_B^2}{m_D^4 \, H_\Sigma} \tag{B-8}$$

and

$$\gamma = \mathrm{Sgn} \underset{\sim}{\boldsymbol{Z}}_\Gamma = - \, \mathrm{Sgn} \underset{\sim}{\boldsymbol{H}}_\Sigma = -\sigma \; . \tag{B-9}$$

These two equations can be combined into

$$\frac{e^{-i\pi\,(2+\gamma)/4}}{\sqrt{|Z_\Gamma|}} = \frac{m_D^2 \sqrt{|H_\Sigma|}}{h_B} \, e^{-i\pi(2-\sigma)/4} \; . \tag{B-10}$$

Using the Fresnel geometrical-spreading formula (B-5), we find

$$\frac{e^{-i\pi\,(2+\gamma)/4}}{\sqrt{|Z_\Gamma|}} = \frac{\cos \alpha_R}{v_R \cos \beta_R} \frac{m_D^2}{h_B} \, \mathcal{L}_F(M_R) \; . \tag{B-11}$$

Substitution of the above expressions into equation (B-7), together with the use of the geometrical-spreading decomposition formula (B-6) and the expression for $\partial_\mu \mathcal{Z}$ given by equation (A-5), leads to

$$I_{as}(\boldsymbol{x}_R, z) = \mathcal{R}(M_R) \, \mathcal{W}_I(\boldsymbol{x}_R, N_R) \, \frac{\cos^2 \alpha_R}{h_B \, v_R^3 \, \cos^2 \theta_R \, \mathcal{L}_S(M_R) \, \mathcal{L}_G(M_R)} \, \delta(z - \Sigma(\boldsymbol{x}_R)) \; . \tag{B-12}$$

We observe that equation (B-12) kinematically reconstructs the singular function (15) of the reflector Σ. To also achieve correct dynamic reconstruction, we have to choose the weight function $\mathcal{W}_I(\boldsymbol{x}_R, N_R)$ such that the amplitude factor in equation (B-12) equals $\mathcal{R}(M_R)$. This determines the sought-for weight function as

$$\mathcal{W}_I(\boldsymbol{x}_R, N_R) = \frac{h_B \, v_R^3 \, \cos^2 \theta_R}{\cos^2 \alpha_R} \mathcal{L}_S(M_R) \mathcal{L}_G(M_R) \; . \tag{B-13}$$

With this choice, we obtain

$$I_{as}(\boldsymbol{x}_R, z) = \mathcal{R}(M_R) \, \delta(z - \Sigma(\boldsymbol{x}_R)) \; , \tag{B-14}$$

Observe that formula (B-14) is just the true-amplitude singular function of the reflector at the chosen point $\boldsymbol{x}_R$. This confirms result (15).

Observing that there is no quantity involved in equation (B-13) that depends on the reflector, we can generalize weight function to any arbitrary point N_Γ. This justifies dropping the subindex R and replacing the stationary point M_R by the generic point M_I on the isochron of M_I. In this way, we arrive to the final weight function of the inverse Kirchhoff integral (11), as stated by equation (12) in the main text.

FIGURE CAPTIONS

FIG. 1: 2-D sketch of a model with reflector Σ and reflection-traveltime surface Γ. Also shown are the isochron and diffraction-traveltime surfaces. Each arbitrary point N_Γ on Γ defines a unique point M_Γ on Σ as the reflection point of ray $SM_\Gamma G$. In the same way, each arbitrary point M_Σ on Σ defines a unique point N_Σ on Γ by the parameter $\boldsymbol{\xi}_\Sigma$ of the source-receiver pair (S_Σ, G_Σ) for which ray $S_\Sigma M_\Sigma G_\Sigma$ constitutes a reflection ray, and by the traveltime along that ray.

FIG. 2: The forward Kirchhoff-Helmholtz integral understood geometrically. For each point M_Σ on Σ, the integration contributes to the reflection response computed for $\boldsymbol{\xi}_R$ at the corresponding point $N_K = (\boldsymbol{\xi}_R, \mathcal{T}(\boldsymbol{\xi}_R, M_\Sigma))$. For details see text.

FIG. 3: The inverse Kirchhoff-Helmholtz integral understood geometrically. For each point N_Γ on Γ, the integration contributes to the reflector depth image computed for $\boldsymbol{x}_R$ at the corresponding point $M_I = (\boldsymbol{x}_R, \mathcal{Z}(\boldsymbol{x}_R, N_\Gamma))$. For details see text.

FIG. 4: Earth model used for the numerical example.

FIG. 5: (a) Synthetic data as modeled by the forward Kirchhoff-Helmholtz integral. (b) Inverted data as obtained by the inverse Kirchhoff-Helmholtz integral.

FIG. 6: (a) Picked peak amplitude in the inverted section of Figure 5b (thin line), as compared with the theoretical reflection coefficient (bold line). (b) Relative error of the amplitudes of part (a).
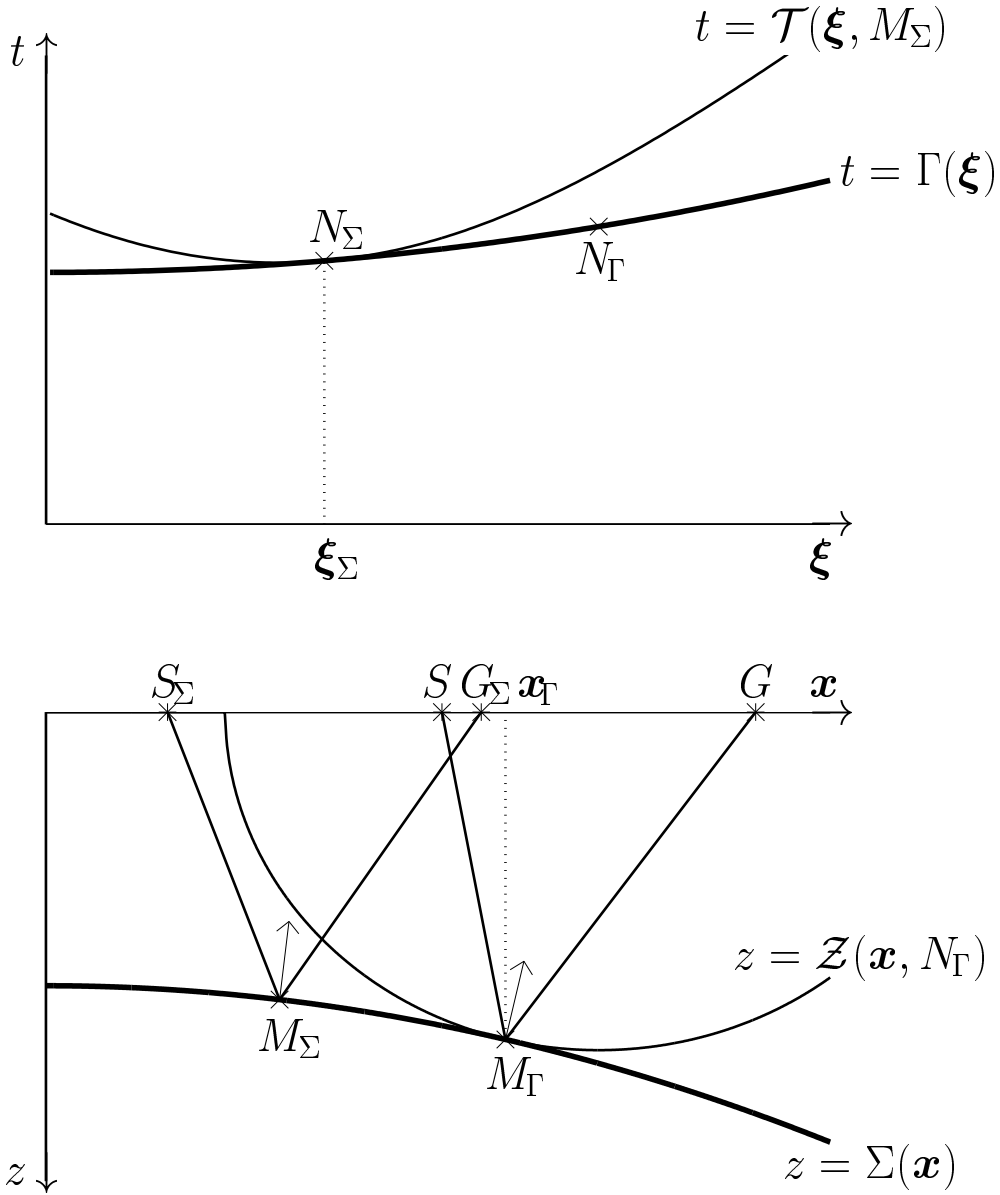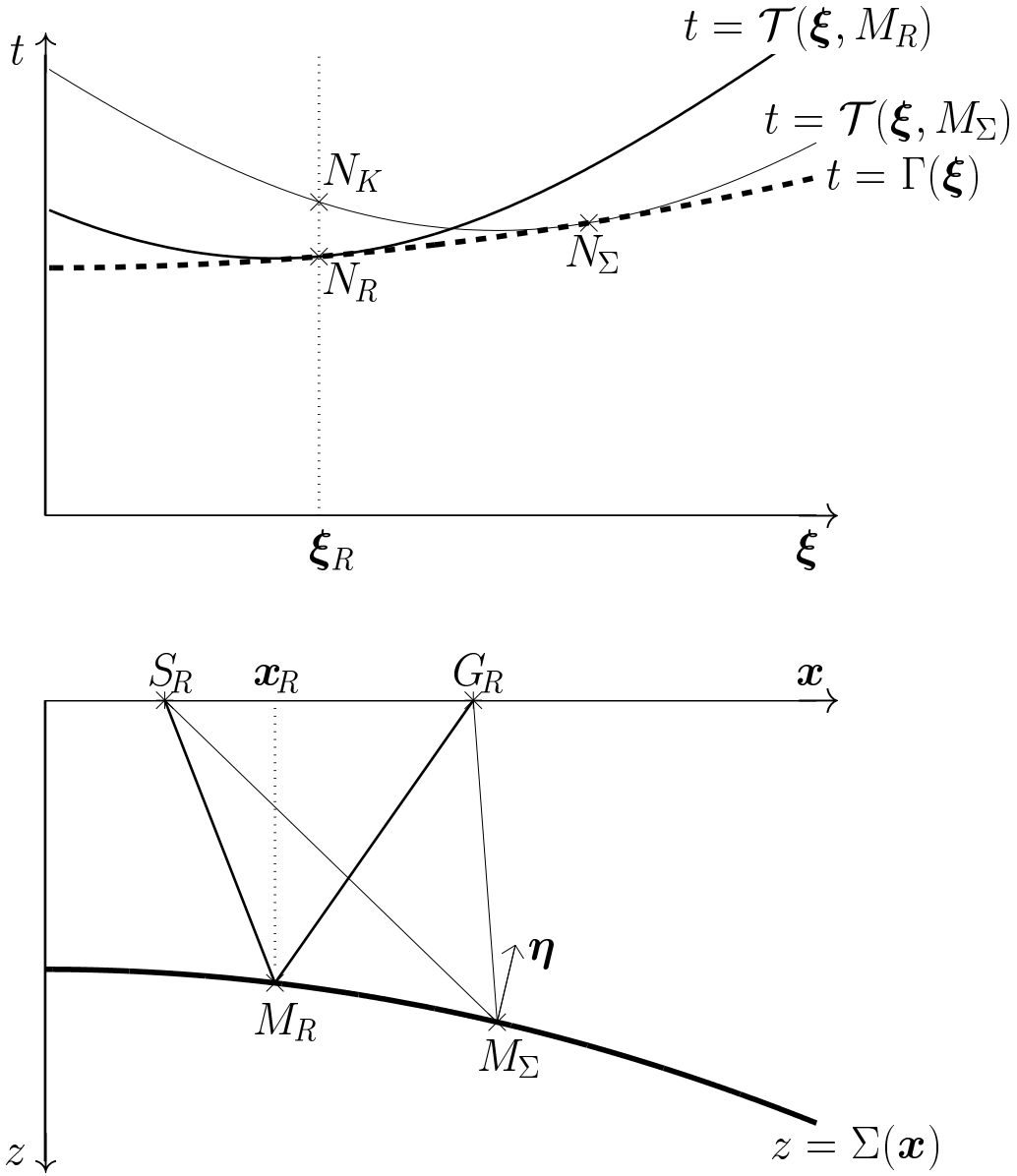
FIG. 1. 2-D sketch of a model with reflector Σ and reflection-traveltime surface Γ. Also shown are the isochron and diffraction-traveltime surfaces. Each arbitrary point N_Γ on Γ defines a unique point M_Γ on Σ as the reflection point of ray $SM_\Gamma G$. In the same way, each arbitrary point M_Σ on Σ defines a unique point N_Σ on Γ by the parameter $\boldsymbol{\xi}_\Sigma$ of the source-receiver pair (S_Σ, G_Σ) for which ray $S_\Sigma M_\Sigma G_\Sigma$ constitutes a reflection ray, and by the traveltime along that ray.
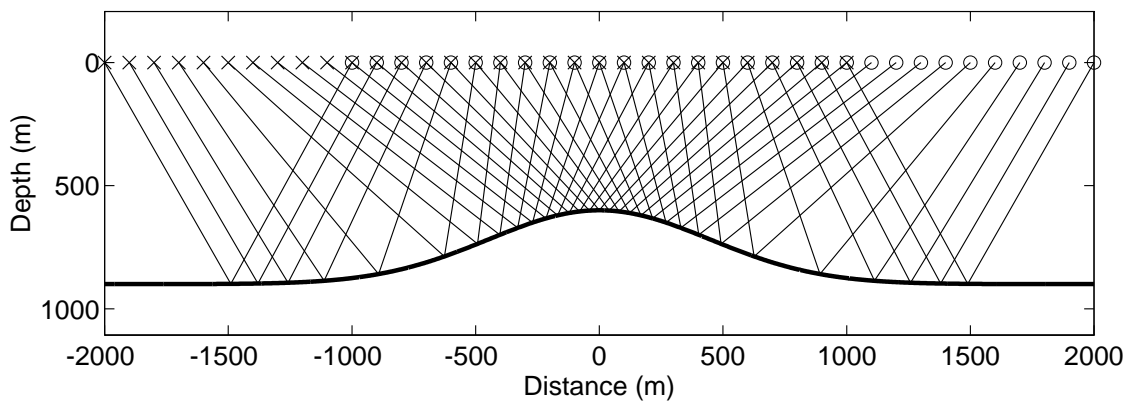
FIG. 2. The forward Kirchhoff-Helmholtz integral understood geometrically. For each point M_Σ on Σ, the integration contributes to the reflection response computed for $\boldsymbol{\xi}_R$ at the corresponding point $N_K = (\boldsymbol{\xi}_R, \mathcal{T}(\boldsymbol{\xi}_R, M_\Sigma))$. For details see text.

FIG. 3. The inverse Kirchhoff-Helmholtz integral understood geometrically. For each point N_Γ on Γ, the integration contributes to the reflector depth image computed for $\boldsymbol{x}_R$ at the corresponding point $M_I = (\boldsymbol{x}_R, \mathcal{Z}(\boldsymbol{x}_R, N_\Gamma))$. For details see text.

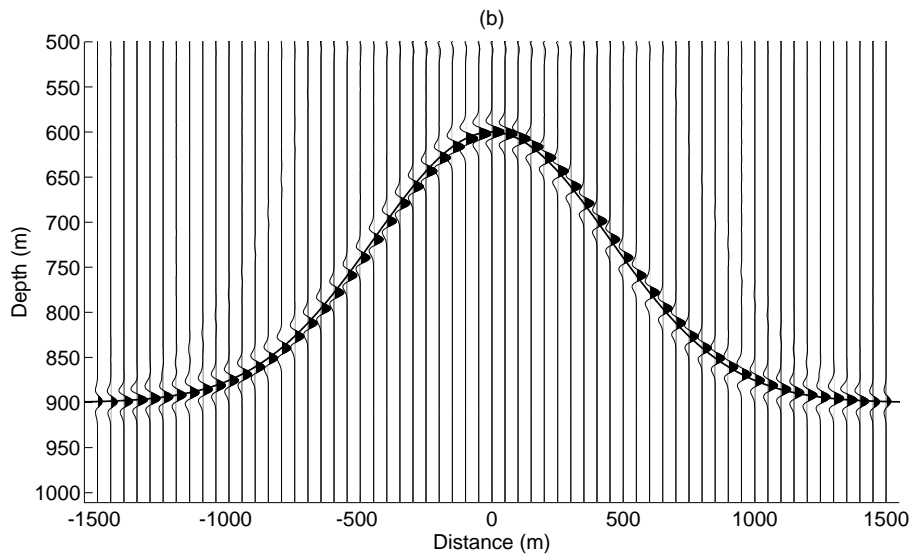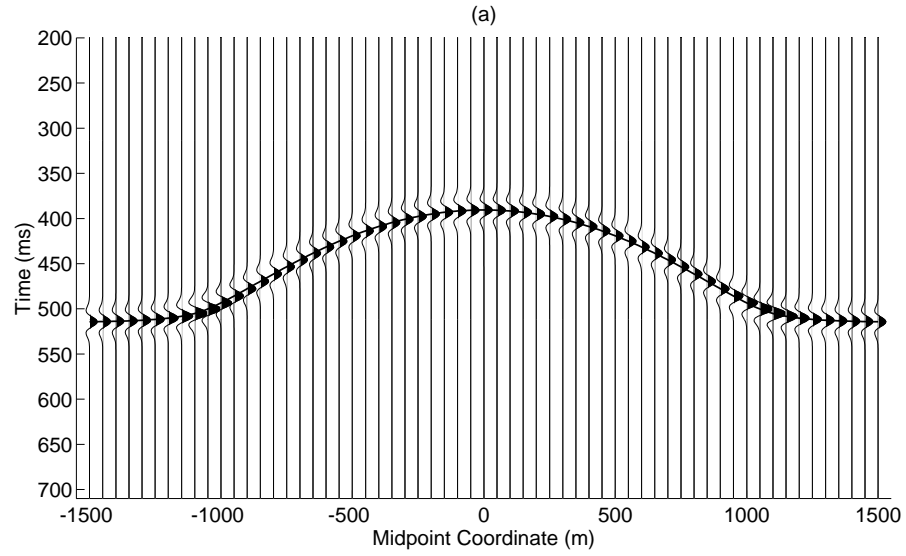FIG. 4. Model for the numerical example.

FIG. 5. (a) Synthetic data as modeled by the forward Kirchhoff-Helmholtz integral. (b) Inverted data as obtained by the inverse Kirchhoff-Helmholtz integral.
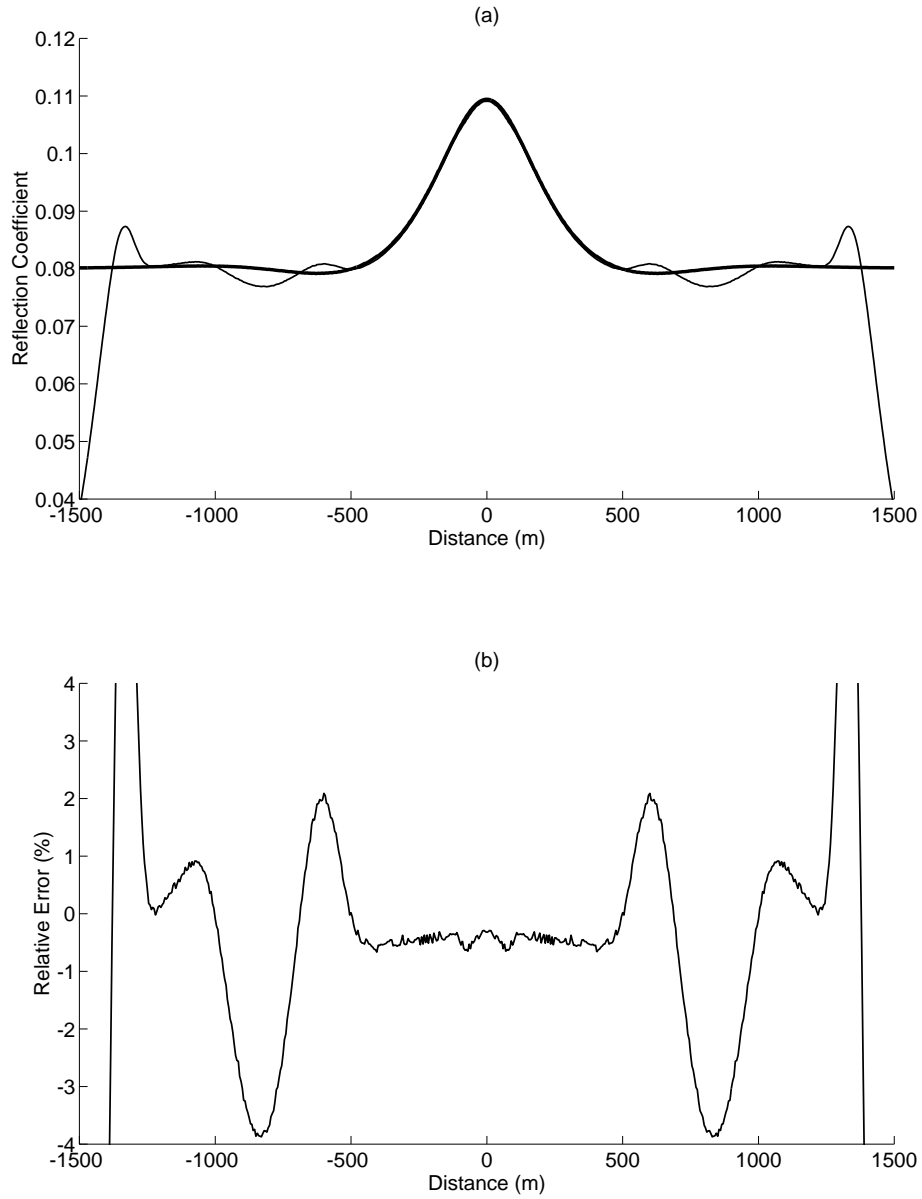
FIG. 6. (a) Picked peak amplitude in the inverted section of Figure 5b (thin line), as compared with the theoretical reflection coefficient (bold line). (b) Relative error of the amplitudes of part (a).

38